Journal of Experimental Botany, Vol. 70, No. 21 pp. 6321–6336, 2019
doi:10.1093/jxb/erz380 Advance Access Publication August 24, 2019
This paper is available online free of all access charges (see https://academic.oup.com/jxb/pages/openaccess for further details)

RESEARCH PAPER

Characterization of the transient fluorescence wave phenomenon that occurs during H_2 production in *Chlamydomonas reinhardtii*

Pilla Sankara Krishna*, Giorgio Morello† and Fikret Mamedov‡

Molecular Biomimetics, Department of Chemistry – Ångström Laboratory, Uppsala University, 751 20 Uppsala, Sweden
*Present address: Department of Molecular Microbiology, John Innes Centre, Norwich NR4 7UH, UK.
†Present address: Inorganic Chemistry Laboratory, Department of Chemistry, University of Oxford, Oxford OX1 3QR, UK.

‡Correspondence: fikret.mamedov@kemi.uu.se

Received 25 January 2019; Editorial decision 13 August 2019; Accepted 14 August 2019

Editor: Nick Smirnoff, University of Exeter, UK

Abstract

The redox state of the plastoquinone (PQ) pool in sulfur-deprived, H_2-producing *Chlamydomonas reinhardtii* cells was studied using single flash-induced variable fluorescence decay kinetics. During H_2 production, the fluorescence decay kinetics exhibited an unusual post-illumination rise of variable fluorescence, giving a wave-like appearance. The wave showed the transient fluorescence minimum at ~60 ms after the flash, followed by a rise, reaching the transient fluorescence maximum at ~1 s after the flash, before decaying back to the initial fluorescence level. Similar wave-like fluorescence decay kinetics have been reported previously in anaerobically incubated cyanobacteria but not in green algae. From several different electron and proton transfer inhibitors used, polymyxin B, an inhibitor of type II NAD(P)H dehydrogenase (NDA2), had the effect of eliminating the fluorescence wave feature, indicating involvement of NDA2 in this phenomenon. This was further confirmed by the absence of the fluorescence wave in the *Δnda2* mutant lacking NDA2. Additionally, *Δnda2* mutants have also shown delayed and diminished H_2 production (only 23% if compared with the wild type). Our results show that the fluorescence wave phenomenon in *C. reinhardtii* is observed under highly reducing conditions and is induced by the NDA2-mediated electron flow from the reduced stromal components to the PQ pool. Therefore, the fluorescence wave phenomenon is a sensitive probe for the complex network of redox reactions at the PQ pool level in the thylakoid membrane. It could be used in further characterization and improvement of the electron transfer pathways leading to H_2 production in *C. reinhardtii*.

Keywords: *Chlamydomonas reinhardtii*, hydrogen production, plastoquinone pool, sulfur deprivation, type II NDH, variable fluorescence.

Introduction

The green alga *Chlamydomonas reinhardtii* is a unicellular model organism, for which a range of methods and techniques for molecular and genetic studies are available (Harris, 2001). It is widely used to study photosynthesis, light perception, respiration, protein synthesis, flagellar structure and function, the cell cycle, and cell–cell interaction. *Chlamydomonas reinhardtii* is also used as a valuable research tool in producing biopharmaceuticals and biofuels (Harris, 2009). Interestingly, in addition to effective oxygenic photosynthesis, *C. reinhardtii* also possess the ability to produce molecular hydrogen (H_2) by its

oxygen- (O_2) sensitive Fe–Fe hydrogenase (HydA) (Horner *et al.*, 2002; Ghirardi *et al.*, 2007), which is probably an evolutionary rudiment of pre-oxygenic metabolism.

Photosynthetically produced H_2 could be considered as the most ideal solar fuel due to its production properties: the use of solar energy, zero CO_2 footprint, use of water as an electron (e^-) and proton (H^+) source, and utilization of photosynthetic light reactions as a driving force (Hankamer *et al.*, 2007; Mathews and Wang, 2009; Kruse and Hankamer, 2010). In *C. reinhardtii*, H_2 can be photoproduced under anaerobic conditions (Gaffron and Rubin, 1942; Healey, 1970; Melis *et al.*, 2000) as a result of PSI-mediated electron transport to plastidial HydA via ferredoxin (Fd) (Evans *et al.*, 1976; Redding *et al.*, 1999; Melis *et al.*, 2000). However, this photoproduction is short lived due to the O_2 sensitivity of the algal HydA. Molecular O_2, co-produced by PSII under illumination, quickly inhibits HydA activity. This creates a challenge to the sustainable, photosynthesis-based H_2 formation in the green algae (Ghirardi *et al.*, 2007; Ghirardi, 2015).

O_2 sensitivity of H_2 production in green algae could be circumvented by complete or partial inhibition of the PSII activity. One of the methods used to achieve this is limitation of *C. reinhardtii* cultures in essential growth nutrients such as S, P, N, and even Mg (Melis *et al.*, 2000; Batyrova *et al.*, 2012; Philipps *et al.*, 2012; Volgusheva *et al.*, 2015). Deprivation of these elements during growth of *C. reinhardtii* produces a similar effect on the photosynthetic reactions, with PSII being the most affected complex. The most commonly used sulfur deprivation (S-dep) (Melis *et al.*, 2000) results in impaired PSII turnover, leading to a decrease in the amount of PSII in the thylakoid membrane. Other effects of S-dep are the increased rate of respiration and accumulation of the reducing equivalents in the cell, leading to accumulation of starch reserves. Typically, after 24–48 h of S-dep, respiration overcomes O_2 evolution by the remaining PSII and anaerobic conditions are established in the cells (Melis *et al.*, 2000; Zhang *et al.*, 2002; Antal *et al.*, 2003; Volgusheva *et al.*, 2013). HydA is activated under these conditions which prevail for a few days, allowing prolonged photoproduction of H_2 up to several days.

There are two major electron sources for H_2 production under S-dep in *C. reinhardtii* (Happe *et al.*, 2002; Fouchard *et al.*, 2005; Ghirardi *et al.*, 2007; Melis, 2007). The first one is photosynthetic and comes from the remaining PSII activity where electrons are extracted from water. The second source is fermentation. Upon establishing anaerobic conditions, *C. reinhardtii* turns its metabolism to fermentation. Therefore, fermentative electron sources become available for the H_2 production in the presence of active HydA (Ohta *et al.*, 1987; Mus *et al.*, 2007). Fermentation of starch contributes to non-photosynthetic transfer of electrons to the plastoquinone (PQ) pool, via a nuclear genome-encoded (*nda2*) and chloroplast-located type II NAD(P)H dehydrogenase (NDA2) as was reported earlier (Mus *et al.*, 2005; Jans *et al.*, 2008; Mignolet *et al.*, 2012; Baltz *et al.*, 2014). Like other type II NAD(P)H dehydrogenase (type II NDH) proteins, *C. reinhardtii*'s NDA2 is the electron only carrier which can reduce the PQ pool from the stromal side (Desplats *et al.*, 2009; Feng *et al.*, 2012). Inhibitor studies in S-dep *C. reinhardtii* cells have confirmed that electrons delivered to HydA are either PSII generated from splitting of H_2O or of stromal origin (Antal *et al.*, 2009).

Both photosynthetic and fermentative electron transport pathways leading to H_2 formation are represented in Fig. 1. Importantly, both pathways coincide at the pool of PQs, the mobile electron carrier inside the thylakoid membrane (Peltier and Cournac, 2002; Peltier *et al.*, 2016). In the presence of light, PSI oxidizes the PQ pool via cytochrome b_6/f complex- (Cyt b_6/f) mediated electron transfer reactions (Fig. 1). PSI produces a significant amount of reduction power (approximately –700 mV) (Ishikita and Knapp, 2003) to reduce stromal protons to H_2 gas in HydA via stromal Fd (–325 mV to –455 mV) (Evans *et al.*, 1976). Therefore, the PQ pool acts as an important intermediate electron carrier to HydA irrespective of the electron source. In addition to that, the PQ pool acts as a redox sensor and is a central point for many other competing electron transfer reactions in the thylakoid membrane of *C. reinhardtii* cells (Peltier and Cournac, 2002; Kruse and Hankamer, 2010; Houille-Vernes *et al.*, 2011).

In cells growing in optimal conditions, the linear electron flow (LEF), driven by both PSII and PSI, dominates in the thylakoid membrane and results in $NAD(P)^+$ reduction which is further utilized in CO_2 assimilation (Fig. 1). It is mediated by stromal soluble Fd and ferredoxin NADP oxidoreductase (FNR) (Batie and Kamin, 1984). In addition to LEF, cyclic electron flow (CEF), which is driven only by PSI, also reduces the PQ pool from reduced Fd either via FNR or via a membrane-associated ferredoxin-quinone reductase (FQR), possibly forming a complex with Cyt b_6/f (Alric, 2014, 2015). CEF promotes formation of ATP by generating the H^+ gradient across the membrane at the expense of NAD(P)H formation. In certain conditions, CEF could contribute up to 50% of the total electron flow in the thylakoid membrane of *C. reinhardtii* (Alric, 2014).

Under S-dep conditions, CO_2 fixation is assumed to be negligible (Melis *et al.*, 2000; Zhang *et al.*, 2002; Hemschemeier *et al.*, 2008) and most of the electrons produced by PSII are delivered to HydA. In contrast, CEF leaks electrons back to the PQ pool, thus impairing H_2 production. Interestingly, in *C. reinhardtii* cells in anoxic conditions with 3-(3,4-dichlorophenyl)-1,1-dimethylurea- (DCMU) inactivated PSII, ~60 electrons are cycled per photosystem per second (Alric, 2014), a number which is comparable with LEF turnover.

Any electron donation to HydA in the thylakoid membrane takes place via the PQ pool which is an entry point for electrons coming from stroma, be it either from fermentation of starch reserves or from NAD(P)H generated by electron transfer from Fd by the activity of FNR (Guedeney *et al.*, 1996; Zhang *et al.*, 2002). The other major fraction of electrons injected into the PQ pool during S-dep originates from the residual water splitting by PSII activity. Both stroma and PSII originated electrons are later passed along the rest of the photosynthetic electron transport chain via Cyt b_6/f and PSI, before being consumed by HydA. In addition, transfer of $NAD(P)^+$/NAD(P)H and other reducing equivalents from mitochondria to chloroplasts or other possible interactions of organelles are also possible (Antal *et al.*, 2009) and is shown in Fig. 1.

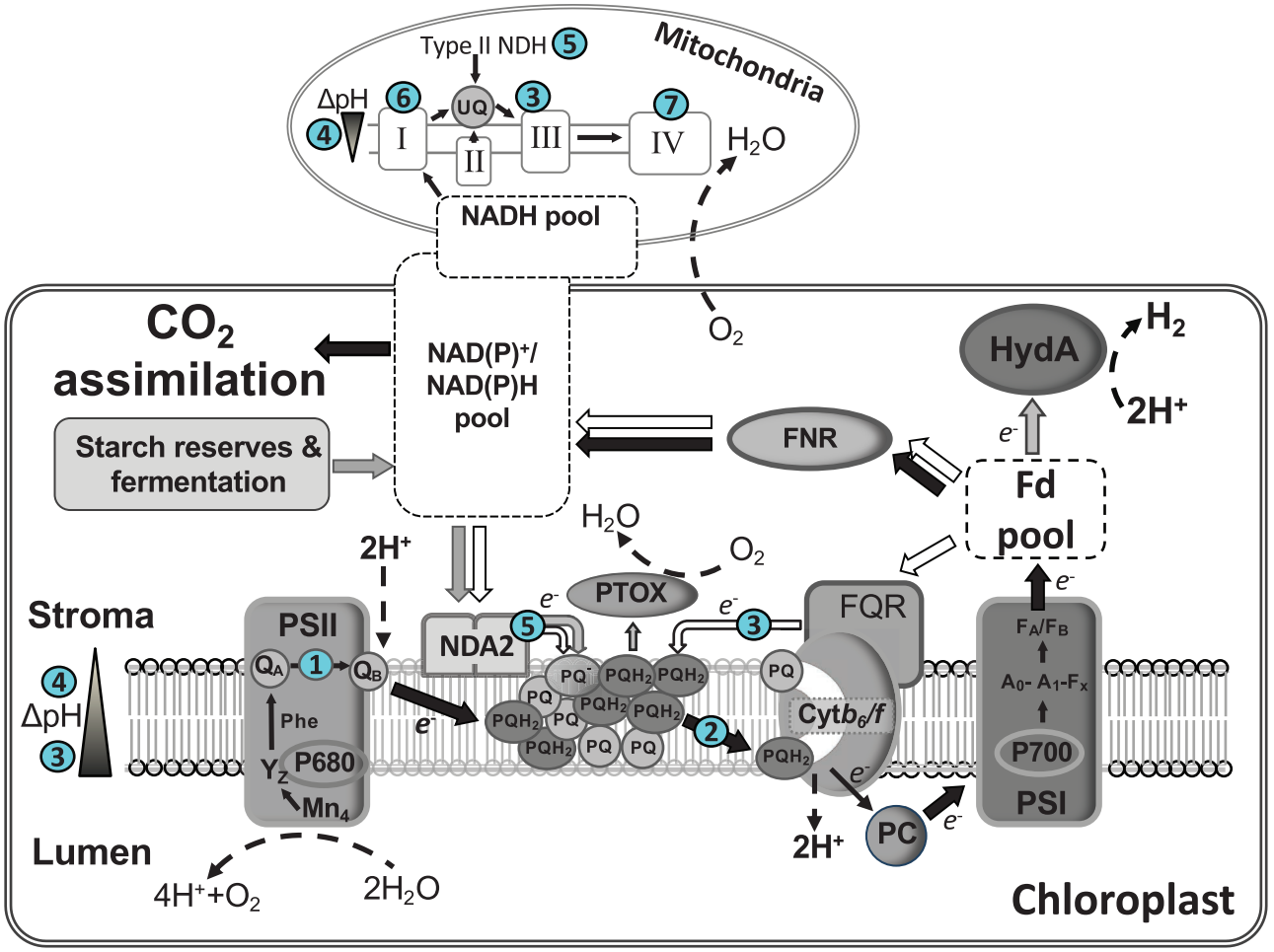

Fig. 1. Schematic representation of the electron and proton transfer pathways leading to H_2 production in *C. reinhardtii* cells under S-dep conditions. Inhibitors used in this study and sites of their action are represented by blue circles with corresponding numbers: DCMU (1), DBMIB (2), antimycin A (3), gramicidin D (4), polymyxin B (5), rotenone A (6), and sodium azide (7). Photosynthetic, fermentative, and CEF pathways are indicated by black, gray, and white arrows, respectively.

The redox state of the PQ pool is an important sensor during different stages of H_2 production, providing information regarding electron and H^+ source for H_2 production. In this study, we used variable fluorescence, originating from PSII and reflecting the redox state of the primary quinone acceptor in PSII (Q_A), as a reporting tool on the redox state of the PQ pool during different stages of H_2 production in *C. reinhardtii* under S-dep conditions. We show that in *C. reinhardtii* cells under highly reducing conditions, such as those required for H_2 production, the specific transient in the variable fluorescence decay after a single flash is observed. This transient fluorescence wave reports on the electron donation from the NDA2 complex, the last electron carrier of the reduced stromal components.

Materials and methods

C. reinhardtii growth conditions and S-deprivation

Wild-type (WT) strains CC406 and CC4533, and the Δ*nda2* mutant strain of *C. reinhardtii* were all grown photoheterotrophically in 1000 ml Erlenmeyer flasks containing 300 ml of standard TAP medium (Gorman and Levine, 1965) at pH 7.0, 25 °C, and constant mixing at 100 rpm. Continuous illumination by white light of intensity of 80 μmol photons m^{-2} s^{-1} was used. After reaching the mid-logarithmic phase at a concentration of 30 μg of chlorophyll (Chl) ml^{-1}, cells were collected by centrifugation at 3000 *g* for 3 min at room temperature and the cell pellet was washed by gentle resuspension with an equal volume of TAP medium without sulfur at pH 7.7 (TAP-S). After three rounds of washing, cells were resuspended in TAP-S medium at a concentration of 15 μg of Chl ml^{-1}. For H_2 evolution experiments, 300 ml of cell suspension in TAP-S were placed in special gas-tight flasks (bioreactors), with 20 ml of air head space. Bioreactors were incubated at 25 °C, 80 μmol photons m^{-2} s^{-1} light, and constant mixing (Volgusheva *et al.*, 2013, 2016). For S-dep experiments under aerobic conditions, *C. reinhardtii* cells, after three rounds of washing in TAP-S, were resuspended at concentration of 15 μg Chl ml^{-1} in 50 ml of TAP-S in 250 ml Erlenmayers flasks with a cotton plug for air exchange under similar temperature, light, and mixing conditions to those above.

Chl concentration and content were measured after extraction in 80% acetone according to Arnon (1949).

PCR confirmation of the Δnda2 mutant

The *C. reinhardtii* WT strain CC4533 and cells lacking NDA2, the *nda2* mutant strain (LMJ.RY0402.206160, Δ*nda2*) with an identified marker cassette (paramomycin resistance cassette) inserted in the 5'-untranslated region (UTR), were obtained from the Chlamydomonas Library Project (CLiP) (Li *et al.*, 2016). Insertional mutation in the *nda2* gene was further confirmed by PCR using NDA2MC F-5' TCAACAGGTCGTGGACATCTTG 3' and Nda2MC R-5'

AACCCCACACGCAGTAGTGTG 3' covering 797 bp upstream and the 1015 bp pre-mRNA coding region of *nda2* from the transcription initiation site. oMJ282 F-5' ATGCTTCTCTGCATCCGTCT 3' and oMJ284 R-5'ATGTTTTACGTCCAGTCCGC 3' primers were used to amplify the control DNA sequence as per CLiP recommendations. Genomic DNA of the WT-CC4533 and Δ*nda2* mutant strain was isolated and PCR was performed with the above-mentioned set of primers and respective genomic DNA as template.

H_2 and O_2 measurement

At the indicated time points, gas samples were collected carefully from the head space of bioreactors through the double septum, using a Hamilton syringe (100 µl) pre-flushed with argon gas. In the H_2-producing stage, starting from 48 h of S-dep onwards, the head space in bioreactors containing an S-dep culture was flushed with argon gas to prevent H_2 back pressure after every measurement. H_2 and O_2 quantifications were done using a Clarus 500 gas chromatograph (PerkinElmer Instruments, Waltham, MA, USA). The peak area of H_2 and O_2 in the GC chromatogram was used to calculate the volume of gas based on standard curves.

H_2 production in the presence of inhibitors

A 25 ml aliquot of *C. reinhardtii* cells after 48 h of S-dep in the H_2-producing stage was taken and placed in 30 ml glass vials, and sealed with a gas-tight butyl rubber seal under O_2-free conditions using a glove box (argon-filled environment and room temperature). Inhibitors were added to the vial before sealing. Gas samples from the head space were collected through the butyl rubber seal after 22 h of incubation at 25 °C under continuous illumination of 80 µmol photons m^{-2} s^{-1} and constant mixing. The amount of H_2 produced with each inhibitor was compared with the amount of H_2 produced in a similar vial without the addition of any inhibitor (control). The following inhibitors were used: 20 µM DCMU, 5 µM 2,5-dibromo-6-isopropyl-3-methyl-1,4-benzoquinone (DBMIB), 4 µM antimycin A, 10 µM gramicidin D, 20 µM rotenone A, 400 µM polymyxin B, and 1 mM sodium azide (see also Table 1).

Measurements of flash-induced variable fluorescence decay kinetics

The flash-induced variable fluorescence decay was measured using a FL3000 dual modulation kinetic fluorometer (Photon System Instruments, Brno, Czech Republic). A saturating actinic flash of 30 µs duration was used, and measuring flashes of 2.5 µs duration were applied as eight per decade in the logarithmic range of 150 µs to 100 s as described in Volgusheva *et al.* (2013, 2016). A 1.5 ml aliquot of *C. reinhardtii* cells was taken at the indicated time points of S-dep and dark adapted for 5 min before the fluorescence decay kinetics were measured. Measurements were done on the culture directly at a concentration of 6×10^6 cells ml^{-1}, corresponding to 15 µg Chl ml^{-1}. All measurements except the control point (0 h of S-dep) were done under anaerobic conditions. Analysis of fluorescence decay kinetics was done using three exponential decay components (Mamedov *et al.*, 2000; Volgusheva *et al.*, 2016). For measurements in the presence of electron or membrane proton gradient inhibitors, the culture was split between two aliquots and the fluorescence kinetics were measured with and without inhibitor, after the cells were incubated in the dark for the time shown in Table 1. The experiments were repeated more than three times, and typical fluorescence traces are shown.

For fluorescence measurements under anaerobic conditions without the S-dep procedure, glucose oxidase (10–25 U ml^{-1}), catalase (60 U ml^{-1}), and 10 mM glucose were added to 1.5 ml of cells grown in standard TAP medium in a special cuvette with an air-tight lid and incubated in the dark for 15 min at room temperature before the measurements.

The flash-induced fluorescence kinetics were analyzed by fitting the multiexponential decay components with an Origin 2016 (OriginLab Corp.).

Results

H_2 production and changes in fluorescence kinetics in S-dep C. reinhardtii *cells*

S-dep results in significant limitation on the photosynthetic reactions in *C. reinhardtii*, especially on the PSII activity. At the beginning of S-dep, the amount of PSII significantly decreases and, as a consequence, the amount of evolved O_2 also decreases, leading to the establishment of anaerobic conditions in the cell culture. Figure 2A (blue circles) shows the amount of O_2 in the gaseous phase of the bioreactor in the course of S-dep. The amount of O_2 decreased from 193.3 µmol to zero, reaching an anaerobic environment during the first ~42 h, and remained at zero for the rest of the experiment (up to 190 h; Fig. 2A, blue circles). With the establishment of anaerobic conditions, the activity of HydA was initiated and H_2 production started and continued for the next 150 h, reaching >10 mmol H_2 l^{-1} of culture (Fig. 2A, red circles).

To study the efficiency of the photosynthetic electron transport under the S-dep conditions, measurements of the flash-induced variable fluorescence decay kinetics (hereafter fluorescence decay) were performed. Variable fluorescence reflects the redox state of Q_A, the primary quinone electron acceptor of PSII (Krause and Weis, 1991; Maxwell and Johnson, 2000). When Q_A is reduced (Q_A^-), the maximal variable fluorescence is observed. Therefore, fluorescence decay after a single flash gives information about all electron transfer processes that lead to the re-oxidation of Q_A^-. The re-oxidation of Q_A^- is usually multiphasic, with individual phases reporting on forward or backward (recombination) electron transfer. The fast phases (µs and ms time range) report on electron transport from Q_A^- to the bound secondary quinone acceptor in PSII (Q_B or Q_B^-) and to the empty Q_B site where Q_B has to bind first. It should be noted that the millisecond phase provides

Table 1. *Electron transfer and membrane proton gradient inhibitors used in this study.*

Inhibitor	Incubation time	Concentration used	Site of action	References
Antimycin A	2 min	4 µM	FQR	Cleland and Bendall (1992); Antal *et al.* (2013)
DBMIB	2 min	5 µM	Cyt b_6/f (Q_O site)	Rich *et al.* (1991); Kurisu *et al.* (2003)
DCMU	2 min	20 µM	PSII (Q_B site)	Bishop (1958); Draber *et al.* (1991)
Gramicidin D	2 min	10 µM	ΔpH and CEF	Rottenberg and Koeppe (1989)
Polymyxin B	5 min	400 µM	NDA2	Mogi *et al.* (2009); Deris *et al.* (2014)
Rotenone A	5 min	20 µM	NDH1	Esposti (1998)
Sodium azide	5 min	1 mM	Cyt IV	Stannard and Horecker (1948)

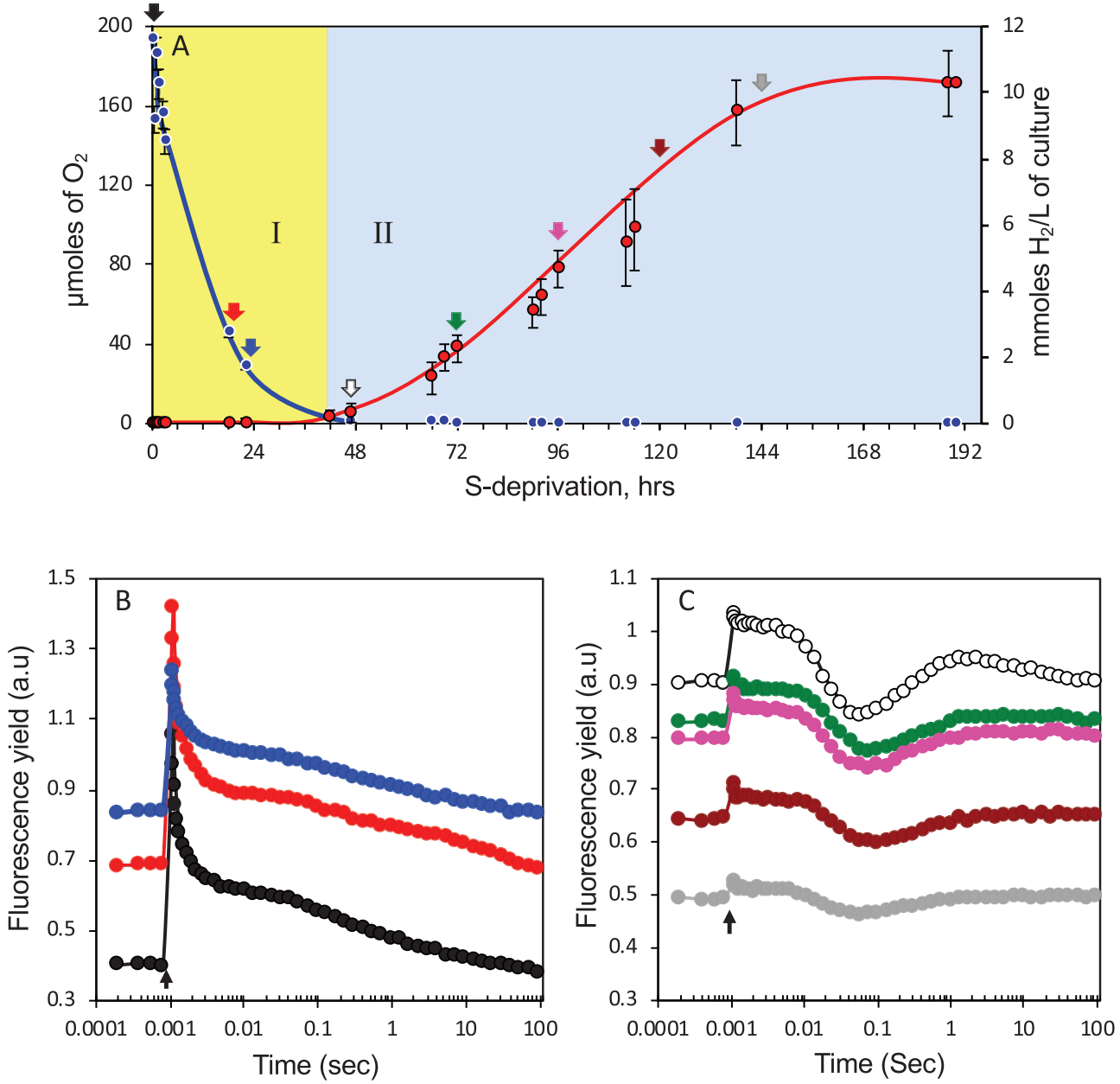

Fig. 2. Changes in the flash-induced fluorescence decay kinetics during S-dep and H_2 production in *C. reinhardtii* cells. (A) The amount of O_2 (blue circles) and photoproduced H_2 (red circles) in the gaseous phase during incubation of *C. reinhardtii* under S-dep conditions in bioreactors. The experiment time course was divided into two stages: O_2 consumption stage (I) and H_2-producing stage (II). The results represent three individual experiments, and the values are the mean values ±SD. The colored arrows (for the color code, see B and C) indicate the time points at which samples were withdrawn for the fluorescence measurements. (B) Flash-induced fluorescence traces measured during the O_2 consumption stage I after 0 h (control, black), 17 h (red), and 24 h (blue) of S-dep. (C) Flash-induced fluorescence decay traces measured during the H_2-producing stage II after 48 h (white), 72 h (green), 96 h (pink), 120 h (brown), and 144 h (gray) of S-dep. Measurements were performed after 5 min of dark adaptation. The time of the actinic flash is indicated with a black arrow.

information on the rate of the PQ molecule binding to the Q_B site in the PSII center, and so effectively reflects the redox state of the PQ pool. The slow phases (hundreds of milliseconds to seconds) reports recombination from Q_A^- to the donor side of PSII (Crofts and Wraight, 1983; Crofts *et al.*, 1993; Renger *et al.*, 1995; Vass *et al.*, 1999; Mamedov *et al.*, 2000; Volgusheva *et al.*, 2016). We have previously reported using flash-induced fluorescence decay kinetics measurements how to assess changes in the photosynthetic electron transfer during S-dep (Volgusheva *et al.*, 2013, 2016).

Fluorescence decay analysis of cells grown under standard conditions in TAP medium or at 0 h of S-dep (Fig. 2B, black trace) reveals three decay phases with the following half-times and amplitudes: the fast phase with $t_{1/2}$ of 424 µs (57%) indicating electron transfer from Q_A^- to Q_B/Q_B^-, the middle phase with $t_{1/2}$ of 7.25 ms (20%) indicating Q_B binding, and the slow phase with $t_{1/2}$ of 1.63 s (23%) indicating recombination to the S_2 state of the water-oxidizing complex in PSII. In our control cells, the fast and efficient forward electron transfer has dominated fluorescence decay after a single flash. The F_v/F_m

ratio (variable fluorescence $F_v=F_m-F_0$), indicative of the PSII efficiency, was found to be 0.62, which is typical for the control S-deprived cells (0 h) after a single flash.

During the O_2 consumption stage I, the initial fluorescence level (F_0) started to increase from 0.40 to 0.70 and to 0.84 after 17 h and 24 h of S-dep, respectively. The maximal fluorescence level (F_m) level first increased from 1.04 to 1.42 and then decreased to 1.24 (Fig. 2B, red and blue traces). As a result, the F_v/F_m ratio decreased from 0.62 to 0.32 during this stage. This suggests a sharp decrease in the PSII activity at the beginning of S-dep. An increase in the F_0 reflects accumulation of Q_A^- (and therefore, 'closed' PSII centers) and a slowdown in the forward electron transfer, as can be seen from the changed kinetics of the fluorescence decay (Fig. 2B, red and blue traces). These results are in line with our earlier reports (Volgusheva *et al.*, 2013, 2016).

Changes in the fluorescence decay kinetics in H_2 production stage II (Fig. 2A) are shown in Fig. 2C. In addition to the one time point reported in Volgusheva *et al.* (2013, 2016) the present study was extended to measurements from five different time points during H_2 production (Fig. 2C). In the beginning of H_2 production, the F_0 level was still high (0.9) and the F_m level was at 1.02, giving an F_v/F_m ratio of 0.12 (Fig. 2C, white trace), which is almost three times smaller than the lowest value, observed at stage I. During the next 96 h of H_2 production, the F_0 level decreased dramatically to 0.49 and the only small variable in fluorescence was observed (F_v/F_m of 0.04, Fig. 2C, gray trace) which is below 10% of the control value. Taken together, these observations indicate that while the amount of PSII with reduced Q_A (Q_A^-) remained high, the total amount of PSII significantly decreased during 192 h of S-dep, which is in agreement with our earlier reports (Volgusheva *et al.*, 2013, 2016).

However, the kinetics of the fluorescence decay during the H_2 production stage were quite different from the kinetics observed in stage I. After a single flash, slow decay with fluorescence reaching below the initial F_0 level with a $t_{1/2}$ of 33 ms was observed (Fig. 2C, white trace). Interestingly, after reaching a minimum at 57 ms, a post-illumination rise in fluorescence yield with a $t_{1/2}$ of 310 ms appeared (Fig. 2C, white trace). After reaching the second maximum following the flash at ~1.7 s, a second, very slow decay of fluorescence with a $t_{1/2}$ of 15 s was observed. This wave-like feature persisted throughout the whole H_2-producing stage II (Fig. 2C). A similar fluorescence wave feature was also observed in the H_2-producing stage during S-dep in the WT-CC4533 strain of *C. reinhardtii* (see below; Fig. 10A).

Fluorescence decay became slightly slower with continued H_2 production, with the $t_{1/2}$ changing from 33 ms to 41 ms and to 78 ms for 48, 72, and 144 h kinetics traces, respectively (Fig. 2C, white, green, and gray traces). The transient minimum of the fluorescence yield also shifted correspondingly from 57 ms to 76 ms and to 101 ms. However, the post-illumination fluorescence rise stayed the same with a $t_{1/2}$ of ~300 ms during all 150 h of H_2 production (Fig. 2C).

This post-illumination rise must reflect backflow of electrons to Q_A in PSII since variable fluorescence reports on its redox state. Therefore, some additional injection of electrons (not from PSII) with a half-time of ~300 ms into the thylakoid membrane, most likely at the level of the PQ pool, must occur after the actinic flash. This injection changes the $Q_A \leftrightarrows Q_B \leftrightarrows PQ/PQH_2$ (PQH_2, dihydroplastoquinone) redox equilibrium even more to the left in the already quite reduced environment.

Fluorescence wave and anaerobic conditions

Deák *et al.* (2014) have reported that incubation of cyanobacterial cells under anaerobic conditions (using the glucose, glucose oxidase, and catalase system) for 15 min resulted in a similar fluorescence wave feature after a single turnover flash. To check if similar treatment is sufficient to induce the fluorescence wave in normal, active *C. reinhardtii* cells, anaerobic conditions were established using the same procedure, and fluorescence decay was measured (Fig. 3). While anaerobic conditions lead to modified fluorescence decay kinetics with much slower fast and middle decay phases [6.9 ms (52%) and 356 ms (14%), respectively] compared with the control cells,

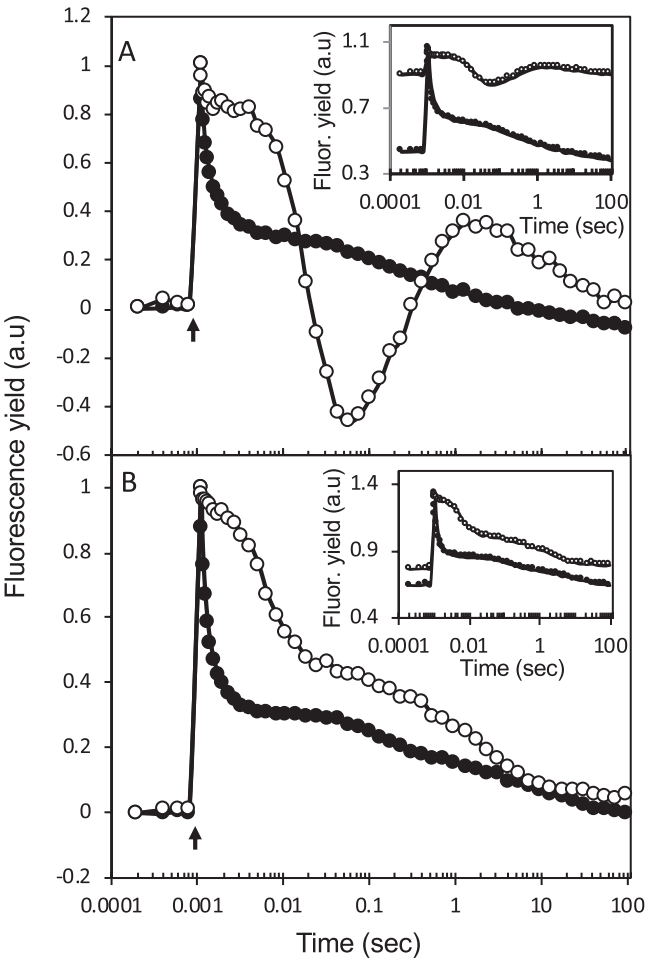

Fig. 3. Effect of anaerobic conditions on the flash-induced fluorescence decay kinetics in *C. reinhardtii* cells. Anaerobic conditions were created either by (A), S-dep (TAP-S) at 0 h (control, ●) and 48 h (○) or (B), by addition of glucose, glucose oxidase, and catalase to the cells grown in regular TAP medium as described in the Materials and methods before (●) and after 15 min of incubation (○). Traces are normalized to the same F_0 and F_m level; non-normalized traces are shown in insets. The time of the actinic flash is indicated with a black arrow.

the fluorescence wave was not observed (Fig. 3B, white trace) as in the case of cyanobacteria (Deák *et al.*, 2014) or as in the case of H_2-producing *C. reinhardtii* cells under S-dep (Fig. 3A). Therefore, anaerobiosis alone is not sufficient to induce the fluorescence wave in fluorescence decay, which indicates different metabolic requirements leading to this phenomenon in *C. reinhardtii*.

PSI-dependent electron transfer is essential in formation of the fluorescence wave

In order to investigate the origin of the fluorescence wave in *C. reinhardtii* during H_2 production, different inhibitors of photosynthetic or mitochondrial electron transport as well as inhibitors of the transmembrane pH gradient (see Table 1) were applied during fluorescence decay measurement. DCMU is a well-known inhibitor of the PSII activity which binds to the Q_B site and effectively blocks forward electron transfer from Q_A^- (Bishop, 1958; Draber *et al.*, 1991). Instead only recombination to the donor side of PSII is reflected in the fluorescence decay (Vass *et al.*, 1999; Mamedov *et al.*, 2000; Roose *et al.*, 2010; Volgusheva *et al.*, 2016). After addition of DCMU, the dominating fast and middle decay phase completely disappeared in the control sample, and only slow recombination between the Q_A^- and the S_2 state was observed (Fig. 4A, black triangles). The result of the DCMU addition to the H_2-producing sample after 48 h of S-dep was very similar (Fig. 4B, white triangles).

DBMIB is another quinone-type inhibitor which binds to the Q_O pocket of Cyt b_6/f, the binding site of PQ, and effectively blocks re-oxidation of the PQ pool (Rich *et al.*, 1991; Kurisu *et al.*, 2003). As expected, in the presence of DBMIB, fluorescence decay kinetics were slower than in the control samples without additions but faster than in the presence of DCMU (Fig. 4A, black squares). This is due to the mix of forward electron transfer (Q_A^- to Q_B/Q_B^-, since some PQ molecules are still available) and recombination reaction (Q_A^- S_2 state). When DBMIB was added to the cells during H_2 production, the fluorescence wave again disappeared, and the result was very similar to the addition of DBMIB to the control sample (Fig. 4B, white squares).

Therefore, inhibition of LEF by addition of either DCMU or DBMIB has abolished the fluorescence wave in the H_2-producing *C. reinhardtii* cells (Fig. 4B). The first result with the DCMU addition was expected, since PSII is effectively cut off from the rest of the electron transport chain. The second result with the addition of DBMIB clearly indicates involvement of the rest of the electron transport chain in the wave formation, most probably PSI.

Inhibition of FQR activity or ΔpH formation led to increased inflow of electrons to the PQ pool

In addition to LEF, PSI also mediates CEF from the PQ pool via the Cyt b_6/f complex and plastocyanin, and back to the PQ pool via FQR or membrane-bound NDA2 (Fig. 1). In green algae, cycling of electrons around PSI significantly increases under anaerobic conditions (Mus *et al.*, 2007). The possible role of CEF in formation of the fluorescence wave was studied

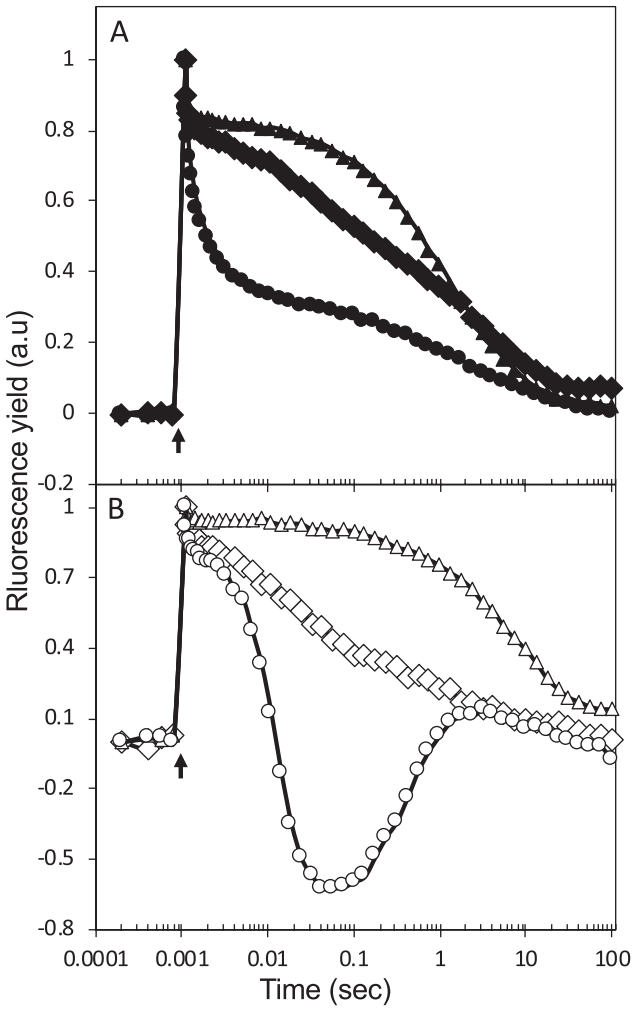

Fig. 4. Effect of inhibitors of the photosynthetic linear electron flow (LEF) on the flash-induced fluorescence decay kinetics of *C. reinhardtii* cells during S-dep. Traces shown are (A), 0 h and (B) 48 h of S-dep with no inhibitor (●, ○), 20 μM DCMU (▲, △), and 5 μM DBMIB (◆, ◇). Traces are normalized to the same F_0 and F_m level. The time of the actinic flash is indicated with a black arrow.

by addition of the inhibitors antimycin A and gramicidin D (Table 1). Under aerobic conditions, inhibition of either FQR by antimycin A (Antal *et al.*, 2013), or of unidentified NDH1 (if any is present in *C. reinhardtii*) by rotenone A (Esposti, 1998), or of the proton gradient across the thylakoid membrane by gramicidin D [a small peptide with the ability to make membrane porous for H^+ (Rottenberg and Koeppe, 1989)] had no effect on the fluorescence decay. In cells grown under normal conditions (control samples), fluorescence decay in the presence of these inhibitors was the same as without additions, and time constants and relative amplitudes of the three decay phases were very similar (not shown). However, in the H_2-producing stage II, the fluorescence decay was significantly affected in the presence of these inhibitors (Fig. 5). Interestingly, incubation of cells with antimycin A or gramicidin D resulted in a rise in F_0, indicating that in the absence of FQR-mediated CEF or a proton gradient across the membrane, the PQ pool is even more reduced (Fig. 5A, inset) in the H_2 production stage II. The wave feature with a post-illumination rise was still present in presence of antimycin A and gramicidin D (Fig. 5A).

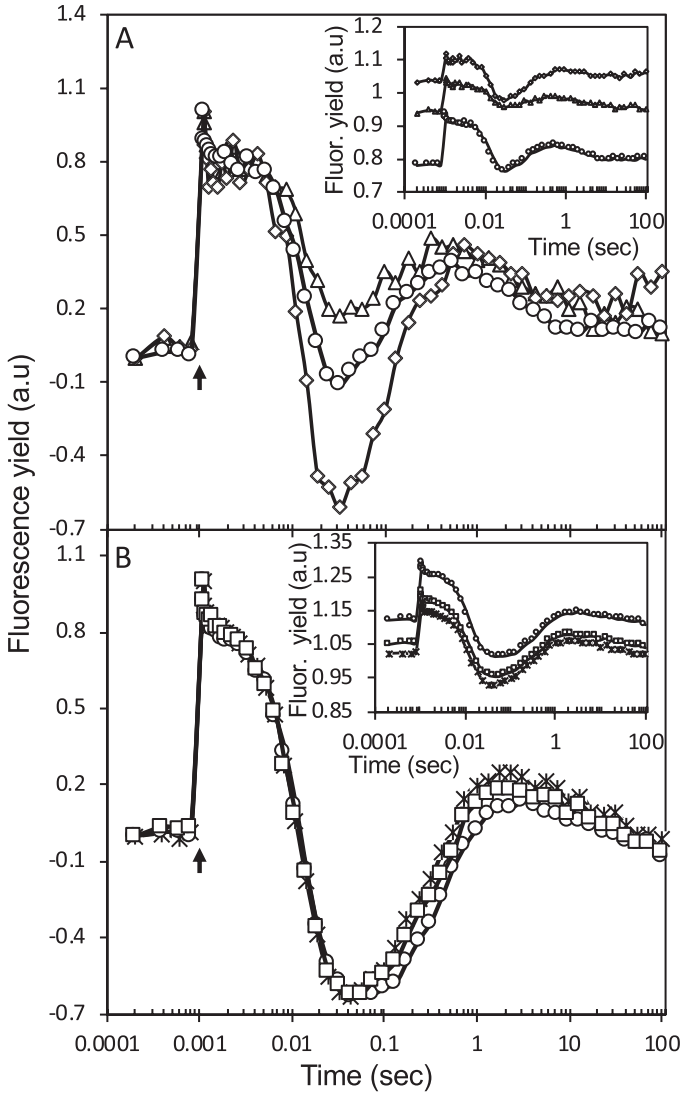

Fig. 5. Effect of inhibitors of the photosynthetic cyclic electron flow (CEF) and proton gradient (A), and mitochondrial electron transport (B) on the flash-induced fluorescence decay kinetics of *C. reinhardtii* cells during S-dep. Traces shown are after 48 h of S-dep with no inhibitor (○), 4 μM antimycin A (△), 10 μM gramicidin D (◇), 20 μM rotenone A (□), and 1 mM sodium azide, 5 (*). Traces are normalized to the same F_0 and F_m level; non-normalized traces are shown in insets. The time of the actinic flash is indicated with a black arrow.

This confirms that the flow of electrons from stromal sources to the PQ pool has increased in the absence of CEF.

Inhibition of mitochondrial electron transfer has no effect on fluorescence decay

Antimycin A and gramicidin D are also known to have inhibitory sites in mitochondrial electron transport (Fig. 1). To differentiate their effect on mitochondrial electron transport from their role in photosynthetic electron transport inhibition, respiratory electron transport inhibitors were used to monitor fluorescence decay during H_2 production in *C. reinhardtii*. Inhibition of mitochondrial Complex I by rotenone A, also a known inhibitor of the type I NDH complex (Mus *et al.*, 2005), or Complex IV by sodium azide was studied. No significant difference was observed in fluorescence decay in the presence or absence of these inhibitors, both in the control cells (not shown) and in the S-dep cells in H_2-producing stage II (Fig. 5B). Thus, a rotenone-sensitive type I NDH does not seem to play a role in the PQ pool reduction and H_2 production in S-dep *C. reinhardtii* cells.

Fluorescence wave is NDA2 dependent

The presence of the type II NAD(P)H dehydrogenase, NDA2, in the thylakoid membrane of *C. reinhardtii* and its involvement in light-independent PQ pool reduction has been reported (Jans *et al.*, 2008; Mignolet *et al.*, 2012; Baltz *et al.*, 2014; Peltier *et al.*, 2016). Based on the functional similarity of this protein to the bacterial homolog, we have studied the effect of polymyxin B addition on fluorescence wave formation. Polymyxin B is a cationic peptide and a specific inhibitor of type II NDH but not type I NDH in Gram-negative bacteria (Deris *et al.*, 2014). *Chlamydomonas reinhardtii* cells were incubated with 400 μM polymyxin B (Table 1) for 5 min in the dark and the fluorescence decay was measured. No significant difference was observed in samples grown in standard TAP medium upon polymyxin B addition (Fig. 6A). However, when S-dep cells in the H_2-producing stage were incubated with polymyxin B, the fluorescence wave feature was completely abolished (Fig. 6B). A drastic decrease in the F_0 level, from 1.24 to 0.73, was observed, almost completely restoring the kinetics to those of the original control (Fig. 6B, inset). Decay kinetics associated with the forward electron transfer from Q_A^- also re-appeared with fast and middle phases [$t_{1/2}$ 423 μs (59%) and $t_{1/2}$ 11 ms (22%) respectively], similar to the control sample (Fig. 6A). Restoration of the normal decay kinetics and disappearance of the wave feature after polymyxin B addition provides strong evidence that the back flow of electrons to Q_A is a result of the electron pressure exerted on the PQ pool via polymyxin B-sensitive NDA2 protein.

Photoproduction of H_2 in the presence of inhibitors

In order to investigate the relationship between the formation of the fluorescence wave and H_2 production, H_2 production was measured in the presence of inhibitors used in this study (Table 1). *Chlamydomonas reinhardtii* cells in the H_2-producing stage at 48 h of S-dep were incubated with different inhibitors for 22 h and the H_2 production was measured directly afterwards. The amount of H_2 produced by cells with no inhibitor (control) was set to 100% and the corresponding amount of H_2 produced by cells incubated with inhibitor was represented in comparison with the control (Fig. 7). In the presence of DCMU, the H_2 yield declined by ~55% which is in good agreement with previously published data (Antal *et al.*, 2009; Volgusheva *et al.*, 2013). Addition of DBMIB almost completely suppressed H_2 production by ~95% (Fig. 7), as has previously been reported (Antal *et al.*, 2009). These data indicate that in *C. reinhardtii* cells the PQ pool is the main point of entry for electrons directed to H_2 production, and the whole process is driven by PSI (Kurisu *et al.*, 2003).

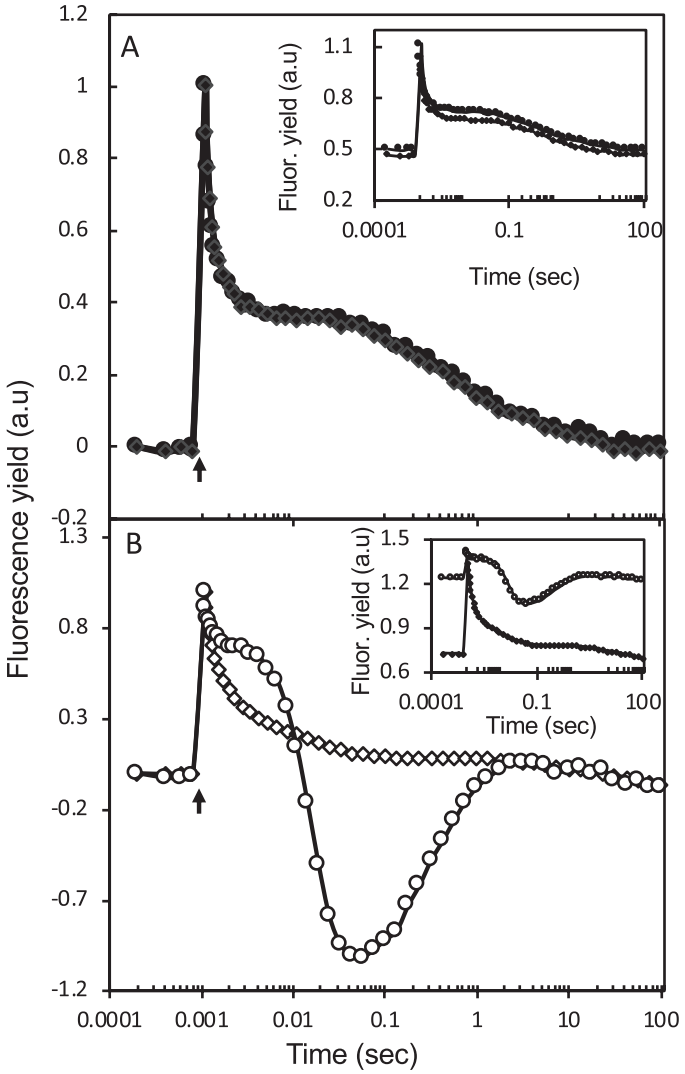

Fig. 6. Effect of inhibition of type-II NDH by polymyxin B on the flash-induced fluorescence decay kinetics of *C. reinhardtii* cells. (A), Cells grown in regular TAP medium with no inhibitor (●) or with 400 μM polymyxin B (◆). (B) Cells after 48 h of S-dep (TAP-S) with no inhibitor (○) or with 400 μM polymyxin B (◇). Traces are normalized to the same F_0 and F_m level; non-normalized traces are shown in insets. The time of the actinic flash is indicated with a black arrow.

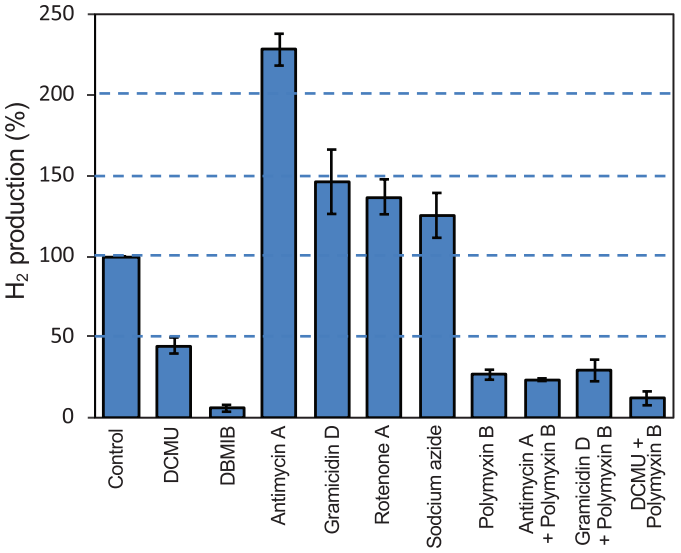

Fig. 7. H_2 production in the presence of the different inhibitors used in this study (Table 1). *Chlamydomonas reinhardtii* cells in the H_2-producing stage at 48 h of S-dep were incubated with different inhibitors, and H_2 production was measured after 22 h of incubation: control (no inhibitor), 20 μM DCMU, 5 μM DBMIB, 4 μM antimycin A, 10 μM gramicidin D, 20 μM rotenone A, 400 μM polymyxin B, and 1 mM sodium azide. Control (no inhibitor) was set to 100%. The presented results were obtained in three individual experiments, and values represented are the mean values ±SD.

In order to evaluate relationships between H_2 formation and FQR-mediated CEF, we examined the effect of antimycin A addition on the amount of H_2 produced by *C. reinhardtii* cells after 48 h of S-dep. Although the effect of antimycin A on CEF is not fully understood and it most probably has multiple targets in the cell (but see Antal *et al.*, 2013), it is clear that its addition increased the amount of produced H_2 >2-fold to almost 230% (Fig. 7), in agreement with results reported earlier (Antal *et al.*, 2009). This result confirms that FQR-mediated CEF might compete with HydA for reduced Fd (Kurisu *et al.*, 2003), as depicted in Fig. 1. Similarly, a positive, but less pronounced effect was observed in the presence of the uncoupler gramicidin D which eliminates the proton gradient across the thylakoid membrane: H_2 production was increased to 146% (Fig. 7).

Other inhibitors of mitochondrial electron transfer such as rotenone A and sodium azide were also tested (Fig. 1). Addition of these compounds facilitated H_2 production in S-dep cells to 137% and 125%, respectively, if compared with the control (Fig. 7). The reason is most likely to be that inhibition of mitochondrial respiration led to the intracellular transfer of NADH to the chloroplast which, in turn, increased the capacity for electron donation via NDA2 (see also (Antal *et al.*, 2009)).

Interestingly, addition of polymyxin B, an inhibitor of NDA2 and the fluorescence wave phenomenon (Fig. 6), resulted in a significant decrease in H_2 production (to only 27%; Fig. 7). Therefore, under S-dep conditions, a significant amount of the electron transport, directed to HydA, is facilitated by NDA2. Those electrons are provided either by starch degradation or by CEF which is driven via FNR functioning as an NAD(P)H-PQ oxidoreductase in *C. reinhardtii* (Desplats *et al.*, 2009) (Fig. 1). We also tested H_2 production in the presence of more than one inhibitor. We observed a clearly increased amount of H_2 produced in the presence of the CEF inhibitors antimycin A and gramicidin D (Fig. 7). When polymyxin B was used together with antimycin A or gramicidin D, the H_2 production dropped to 23% and 29%, respectively, similar to the inhibition by polymyxin B alone (27%; Fig. 7). This indicates that additional inhibition of CEF is not relevant when NDA2 is already inhibited by polymyxin B. Moreover, when polymyxin B was used together with DCMU, a significant reduction in the H_2 production to 12% was observed (Fig. 7). This residual H_2 production when both known electron sources are inhibited suggests that some alternative modes of electron donation are still present in the S-dep *C. reinhardtii*.

A proton gradient is not required for formation of the fluorescence wave

S-dep cells in the H_2-producing stage exhibit a wave feature in the fluorescence decay kinetics. This phenomenon is observed

under anaerobic conditions created by the S-dep procedure (Fig. 1A). If the same cells were exposed to open air, no fluorescence wave was observed (not shown). Therefore, in the presence of O_2, electron pressure on the PQ pool is relieved, most probably by plastid terminal oxidase (PTOX) present in the thylakoid membrane of *C. reinhardtii* (Fig. 1; Johnson and Alric, 2013). Similarly, cells that were grown in TAP-S under aerobic conditions did not exhibit any wave feature in the fluorescence decay (Fig. 8A). However, when anaerobic conditions were created by the addition of glucose, glucose oxidase, and catalase to S-dep cells grown for 42 h under aerobic conditions (Fig. 8B, circles), fluorescence decay became slower and the appearance of small wave-like feature could be noted (Fig. 8B, diamonds). When gramicidin D was added to the same cells, a fully developed fluorescence wave was clearly observable (Fig. 8B, triangles). This result shows that the absence of a ΔpH across the membrane facilitates increased inflow of electrons to the PQ pool and, correspondingly, the increased H_2 production in S-dep *C. reinhardtii* cells.

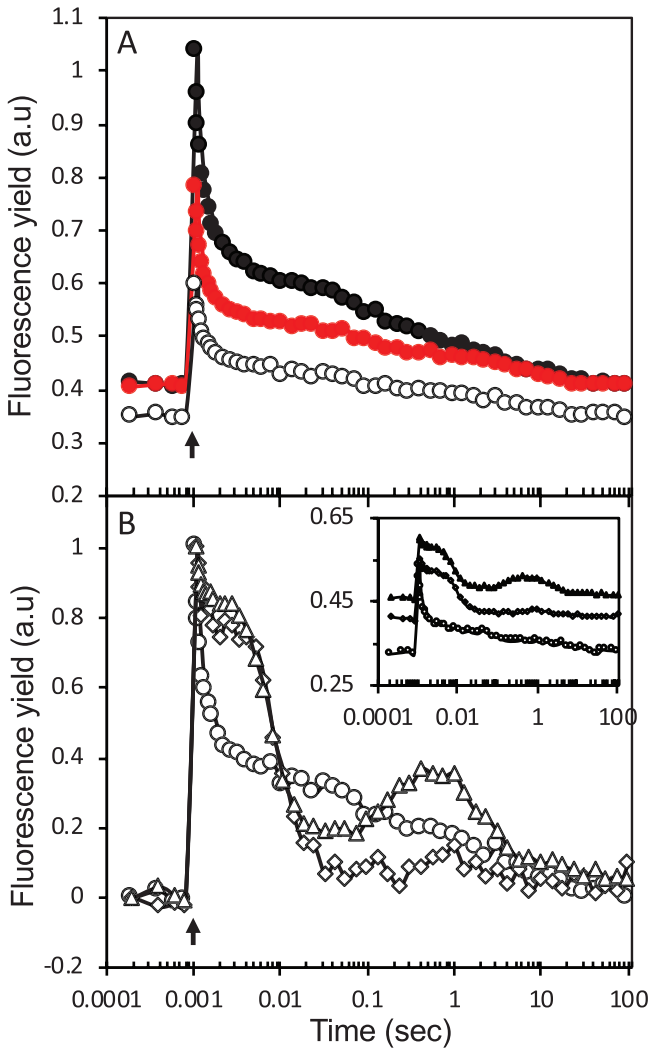

Fig. 8. Effect of gramicidin D, a proton gradient inhibitor, on the flash-induced variable fluorescence decay kinetics of *C. reinhardtii* cells under different anaerobic conditions. (A) S-dep cells incubated under aerobic conditions for 0 h (black), 17 h (red), and 42 h (white). (B) S-dep cells incubated under aerobic conditions for 42 h with no addition (○), or further incubated for 15 min after addition of glucose, glucose oxidase, and catalase in the absence (◇) or presence of gramicidin D (△). Traces are normalized to the same F_0 and F_m level; non-normalized traces are shown in insets. The time of the actinic flash is indicated with a black arrow.

H_2 production and fluorescence decay kinetics in the S-dep Δnda2 mutant in C. reinhardtii

In order to further establish that NDA2 is involved in formation of the fluorescence wave in S-dep *C. reinhardtii*, the *nda2* knockout mutant (Δ*nda2*) from the *Chlamydomonas* mutant library (CLiP, www.chlamylibrary.org) was tested. Figure 9A shows the PCR products resolved on a 1% agarose gel. WT genomic DNA as a template was amplified by primers for the control gene as well as for *nda2* with the specific primers at an expected size on the gel (Fig. 9A, WT lanes C and N). In contrast, Δ*nda2* genomic DNA did not result in any amplification for *nda2*, but it did for the control gene (Fig. 9A, Δ*nda2* lanes C and N), indicating disruption of the gene with insertion of the marker cassette.

Δ*nda2* mutant cells and the corresponding WT-CC4533 were pre-cultured and subsequently subjected to the S-dep procedure as before, and O_2 and H_2 concentrations in the gaseous phase were measured during the first 164 h (Fig. 9B, C). Figure 9B (blue circles) shows the amount of O_2 in the gaseous phase of the bioreactor during S-dep of WT-CC4533. Similar to the WT-CC406 strain (Fig. 2A), WT-CC4533 exhibited two stages: the O_2 consumption stage I and the H_2-producing stage II, although stage I was slightly shorter and the amount of H_2 produced during stage II was ~40% lower (5.84±0.25 mmol l^{-1} of culture) (Fig. 9B, red circles) than that of WT-CC406 (10.27±0.99 mmol, Fig. 2A, red circles). Interestingly, in the given conditions, the Δ*nda2* mutant showed an initial increase in the O_2 concentration in the gaseous phase of the bioreactor, followed by O_2 consumption and H_2-producing stages (Fig. 9C, blue circles, green fill area). This resulted in much later (by 72 h if compared with WT-CC4533) establishment of anaerobic conditions at 88 h of S-dep (Fig. 9B, C), and the concentration of O_2 remained at zero level during the rest of the experiment (stage II; Fig. 9C). During stage II, the Δ*nda2* mutant cells produced only 1.29±0.37 mmol of H_2 l^{-1} of culture, which is only 23% of H_2 gas produced by the corresponding WT-CC4533 strain (Fig. 9B, C).

Fluorescence decay was measured in the course of the experiment. At 0 h of S-dep, both WT-CC4533 and Δ*nda2* mutant cells exhibited typical flash-induced fluorescence decay kinetics reflecting fast forward electron transfer from Q_A^- (Fig. 10A, B, black trace). With continued S-dep, a rise in F_0 and F_m was observed along with the increasingly slower decay kinetics, indicating the appearance of sequentially more reducing conditions in the thylakoid membrane similar to WT-CC406 cells as presented earlier in Fig. 2A. When WT-CC4533 cells reached H_2-producing stage II, fluorescence kinetics exhibited the typical fluorescence wave feature as described above (Fig. 10A, white trace). The wave feature was persistent throughout the whole H_2-producing stage in WT-CC4533 cells, like the fluorescence kinetics in WT-CC406 cells shown in Fig. 2C.

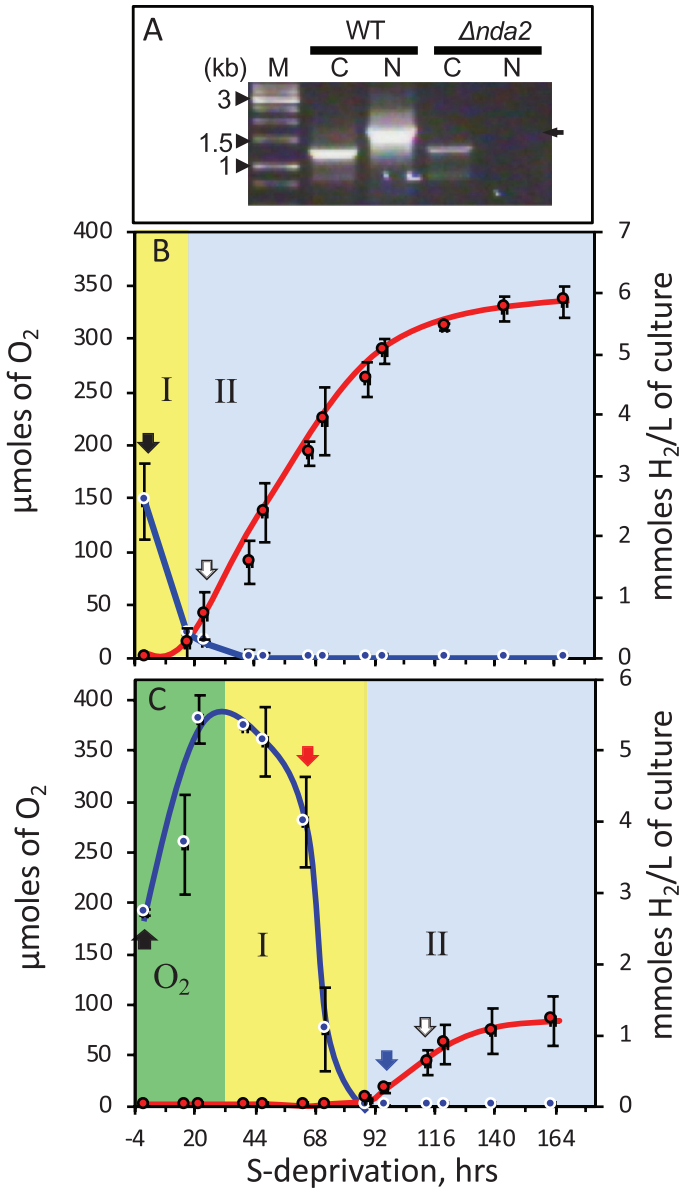

Fig. 9. S-dep and H_2 production in the Δ*nda2* mutant and WT-CC4533 strains of *C. reinhardtii*. (A) Genomic PCR analysis with the primers NDA2MC F and NDA2MC R for *nda2*, N, and with the primers oMJ282 F and oMJ284 R for the control gene, C; M, 1 kb DNA ladder; Δ*nda2*, PCR product with Δ*nda2* DNA as a template; WT, PCR product with wild-type genomic DNA as a template. Changes in the amount of O_2 (blue circles) and photoproduced H_2 (red circles) in the gaseous phase during incubation of the *C. reinhardtii* WT-CC4533 cells (B) and the Δ*nda2* mutant cells (C). In addition to the O_2 consumption stage I and the H_2-producing stage II, the O_2-producing stage was observed in the Δ*nda2* mutant. The results represent three individual experiments, and values represented are the mean values ±SD. The colored arrows (for the color code, see Fig. 10A and B, respectively) indicate the time points where samples were withdrawn for the fluorescence measurements.

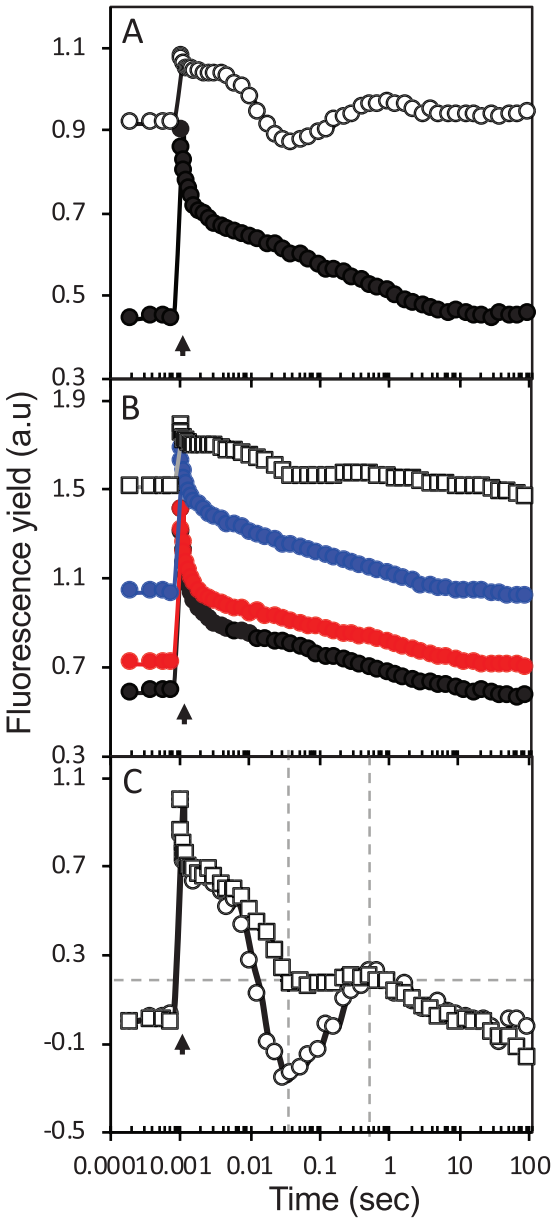

Fig. 10. Flash-induced fluorescence decay traces measured during S-dep of *C. reinhardtii* cells in the WT-CC4533 cells (A) after 0 h (black) and 24 h (white) (see Fig. 9B) and in the Δ*nda2* mutant cells (B) after 0 h (black), 65 hrs (red), 96 h (blue), and 113 h (white) (see Fig. 9C). (C) Comparison of the normalized fluorescence decay kinetics from the H_2-producing WT-CC4533 cells (24 h of S-dep, ○) and the Δ*nda2* mutant cells (113 h of S-dep, □). The time of the actinic flash is indicated with a black arrow.

Interestingly, the Δ*nda2* mutant cells do not exhibit a clearly distinguishable wave feature in fluorescence kinetics even after 96 h of S-dep and 24 h of the H_2 production stage (Figs 9C, 10B). The decay kinetics became gradually slower and, after 113 h of S-dep, fluorescence kinetics were dominated by a slow middle decay phase with a $t_{1/2}$ of 32 ms and a delay of the slow recombination phase which can be considered a residue of the post-illumination rise (Fig. 10B, white trace). Comparison of fluorescence kinetics from the WT-CC4533 after 24 h of S-dep and from the Δ*nda2* mutant after 113 h of S-dep under similar H_2-producing conditions is shown in Fig. 10C. Thus, the absence of the fluorescence wave correlates with the lack of NDA2 and low H_2 production in the Δ*nda2* mutant of *C. reinhardtii*.

Discussion

Chl fluorescence has been widely used to study changes in the photosynthetic electron transfer during H_2 production in S-dep *C. reinhardtii*. The measurements typically include *in situ*

monitoring of F_m and F_0 parameters (Wykoff *et al.*, 1998; Antal *et al.*, 2006, 2007; Faraloni and Torzillo, 2010; Godaux *et al.*, 2013; Deák *et al.*, 2014), excitation energy transfer (Volgusheva *et al.*, 2007), and variable fluorescence induction (Antal *et al.*, 2003, 2010; Kosourov *et al.*, 2007; Makarova *et al.*, 2007; Volgusheva *et al.*, 2007). Among these, the flash-induced variable fluorescence decay measurements are most informative since they are able to provide kinetic information about electron transfer between PSII and the PQ pool, the focal point of electron transport pathways in *C. reinhardtii* (Volgusheva *et al.*, 2013, 2016). In this work, we demonstrate for the first time that in *C. reinhardtii* cells under S-dep H_2-producing conditions, after a single flash, the fluorescence kinetics reproducibly exhibit a wave-like phenomenon (Fig. 2C). The fluorescence wave consists of an initial decay with a $t_{1/2}$ of 33 ms, to the level below F_0 which existed before the flash, and a consequent rise with a $t_{1/2}$ of ~300 ms recovering almost half of F_v (Figs 2C, 3A). This wave phenomenon reflects backward electron transfer to PSII as a result of shifted equilibrium between the PQ pool and quinone acceptors in PSII ($Q_A^- \Leftarrow Q_B \Leftarrow PQ/PQH_2$) after an additional post-illumination injection of electrons to the already reduced PQ pool during H_2 production.

A similar fluorescence wave phenomenon was observed in *Synechocystis* PCC 6803 and several other cyanobacterial species (Deák *et al.*, 2014). However, in cyanobacteria, fluorescence phenomenon was induced after applying microaerobic conditions to the normally grown cells (i.e. after incubation with a glucose, glucose oxidase, and catalase mixture for 15 min) (Deák *et al.*, 2014).

High reduction level of the PQ pool is a requirement for the appearance of the wave feature

A significant increase in the F_0 level during the first 48 h of S-dep indicates accumulation of Q_A^- in the majority of the PSII centers which, in turn, reflects the over-reduction of the PQ pool (Fig. 2B, C). The consequent decrease in the F_0 level during the next 144 h reflects an overall decrease in the amount of PSII rather than re-oxidation of Q_A^- (Fig. 2C) (Volgusheva *et al.*, 2013, 2016). As a result of the over-reduced state of the PQ pool, these remaining PSII centers mostly contain an empty Q_B site and show slow fluorescence decay (with a $t_{1/2}$ of 30–80 ms) as a first part of the wave feature (Fig. 11, II). This finding leads to the conclusion that the increased reduction level of the PQ pool is an important pre-condition for the fluorescence wave formation in *C. reinhardtii* cells.

This reduction level in *C. reinhardtii* cells must be higher than in cyanobacteria. Application of the microaerobic conditions alone was not enough to induce a fluorescence wave in *C. reinhardtii* (Fig. 3B). It is known that S-dep induces a change in the redox state in the cells. The redox potential in the TAP-S medium drops by 500 mV (from 400 mV to −100 mV) during transition to anaerobiosis (Kosourov *et al.*, 2002; Antal *et al.*, 2003). Addition of glucose, glucose oxidase, and catalase removes O_2 from the medium and creates microaerobic conditions in the cells but does not change the E_m potential to the same extent. Another important difference between the species is that *C. reinhardtii* have a different network of electron

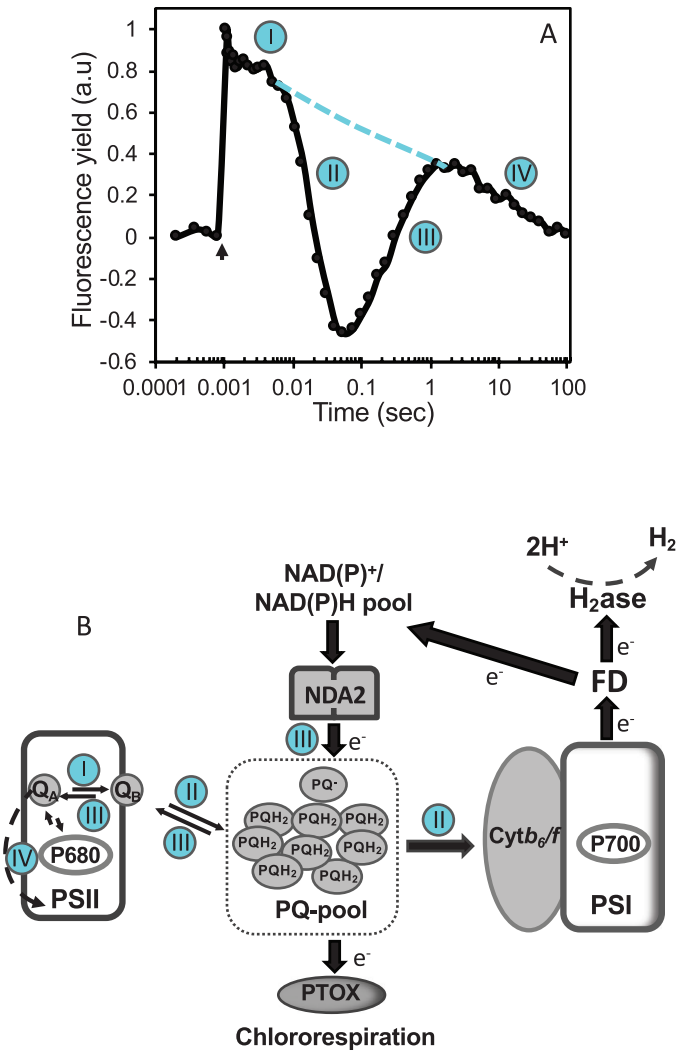

Fig. 11. Proposed scheme (B) to explain different phases (A) during the transient fluorescence wave phenomenon at the H_2-producing stage in *C. reinhardtii* (see Conclusions for explanation).

transfer reactions in and from the PQ pool, some of which could contribute to the wave formation (Houille-Vernes *et al.*, 2011) (Fig. 1).

Importantly, if the reduction of the PQ pool by PSII is inhibited by the addition of DCMU, PSII is completely isolated from the rest of the thylakoid membrane components and cannot serve as a fluorescence probe for the redox changes in the PQ pool, so no fluorescence wave feature is observed (Fig. 4). If the oxidation of the PQ pool by PSI is inhibited by the addition of DBMIB, again no fluorescence wave feature was observed (Fig. 4). Therefore, even in the highly reduced state, the PQ pool still serves as a focal point of the light-induced electron transport reactions and must be open from both reductive and oxidative sides for formation of the fluorescence wave.

PSI is essential for the formation of a fluorescence wave

The previous observation with addition of DBMIB points to the essential role of PSI in the formation of a wave as part of LEF. DBMIB binds to the Q_O site of the Cyt b_6/f complex

where re-oxidation of PQH_2 occurs, thereby preventing further electron transport towards PSI (Kurisu *et al.*, 2003). A single turnover flash activates both PSII- and PSI-mediated electron transfer. In the case of an imbalance between PSII and PSI towards PSI, which takes place during S-dep, partial oxidation of the PQ pool takes place. This re-oxidation of the PQ pool by PSI via Cyt b_6/f must occur more rapidly than 30 ms in order to create the 'redox space' in the PQ pool for the slow re-reduction from PSII, which is observed as slow Q_A^- re-oxidation (slow fluorescence decay, first part of the wave with a $t_{1/2}$ of 33 ms; Fig. 11, I and II). This event is inhibited by the addition of DBMIB and, as a result, the fluorescence wave is not observed (Fig. 4B).

PSI also drives CEF (Cleland and Bendall, 1992; Alric, 2014) which contributes to the PQ pool reduction and proton gradient across the thylakoid membrane while strongly competing with the electron supply to HydA (Tolleter *et al.*, 2011). Addition of antimycin A or gramicidin D, in addition to dissipation of ΔpH, may also affect CEF since it is clear that the H_2 production was strongly increased in their presence (Fig. 7). Moreover, the fluorescence wave with an elevated level of F_0 was also still present (Fig. 5A, inset). Therefore, the PQ pool was probably even more reduced in the absence of ΔpH, and PSI was more active in this case. In addition, it increases the availability of H^+ on the stromal side for both PQ pool reduction and HydA activity.

Fluorescence wave phenomenon in C. reinhardtii *requires a different, NDA2-mediated electron transfer pathway*

So far the conditions under which the fluorescence wave was observed in *C. reinhardtii* were quite similar to those observed in cyanobacteria – a highly reduced PQ pool and PSI-mediated electron transfer (Deák *et al.*, 2014). The only difference so far is that the PQ pool must be even more reduced in *C. reinhardtii* and this is achieved by S-dep, where anaerobiosis could be established either by incubation of S-dep cultures in sealed bioreactors (Fig. 2) or by addition of a microaerobic mixture (Fig. 8). In both cases, the fluorescence wave phenomenon is observed (Figs 2C, 8B).

Another condition for formation of the fluorescence wave in cyanobacteria is the electron flow from the reduced stromal components mediated by the NDH1 complex (Deák *et al.*, 2014). However, we observed no effect of rotenone A, a known inhibitor of NDH1 (Esposti, 1998), on formation of the fluorescence wave (Fig. 5B). Therefore, another electron transfer pathway, not involving the NDH1 complex, must be relevant in *C. reinhardtii*. Moreover, the existence of NDH1 in *C. reinhardtii* has not been demonstrated at the molecular level (Desplats *et al.*, 2009). Instead, the rotenone A-insensitive NDA2 protein was proposed to mediate the electron flow towards the PQ pool in *C. reinhardtii* chloroplasts (Jans *et al.*, 2008; Desplats *et al.*, 2009; Mignolet *et al.*, 2012; Baltz *et al.*, 2014). It was also shown that silencing of NDA2 encoded by the *nda2* gene decreased the H_2 production under S-dep in *C. reinhardtii* (Jans *et al.*, 2008). NDA2 could be inhibited by polymyxin B, similar to type II NDH of multidrug-resistant pathogenic bacteria such as *Mycobacterium smegmatis* (Mogi *et al.*, 2009; Deris *et al.*, 2014). Accordingly, addition of polymyxin B completely abolished the appearance of the wave in the fluorescence kinetics in *C. reinhardtii* cells during the H_2-producing stage (Fig. 6B). Addition of polymyxin B not only eliminated this fluorescence transient but also significantly decreased the F_0 level (Fig. 6B, inset). Therefore, our data clearly show that in the presence of polymyxin B, the NDA2-dependent inflow of electrons is absent, resulting in the more oxidized state of the PQ pool.

Our conclusion that NDA2 is necessary for formation of the fluorescence wave and mediation of the electron flow from the reduced components of stroma to the PQ pool was confirmed by measurements in the *Δnda2* mutant. Under S-dep, *Δnda2* cells produced five times less H_2 than the corresponding WT cells (23%; Fig. 9B, C), similar to that reported by Mignolet *et al.* (2012) using *nda*-RNAi. The offset of anaerobiosis, and consequently the H_2 production, were significantly delayed in the mutant (by 72 h; Fig. 9B, C) and no fluorescence wave feature was observed even after >100 h of S-dep (Fig. 10B). Therefore, our data confirm that NDA2, calcium-dependent type II NDH, significantly contributes to the H_2 production by donating electrons to the PQ pool and is necessary for the formation of the fluorescence wave in S-dep *C. reinhardtii*. This NDA2-mediated electron transfer occurs with a $t_{1/2}$ of 310 ms and is observed as a transient rise in the fluorescence wave (Fig. 11, III).

Conclusion

Our results demonstrate that during H_2 production, S-dep *C. reinhardtii* cells exhibit a transient wave phenomenon in the flash-induced fluorescence decay kinetics. Important pre-conditions required for the occurrence of this phenomenon are: (i) a high degree of reduction of the PQ pool; (ii) functional PSI which can drive oxidation of the PQ pool via Cyt b_6/f; and (iii) undisturbed electron flow from the reduced stromal components, mediated by the NDA2 protein. Among those, the state of the PQ pool is a key pre-condition not only because it must be more reduced than in cyanobacteria, but also because the PQ pool is a crucial focal point of multifaceted redox reactions and ΔpH regulation, some of which are directed to H_2 production (Fig. 1).

Figure 11 shows a proposed scheme of electron transfer reactions leading to fluorescence wave formation during H_2 production in *C. reinhardtii* cells. Different decay phases and corresponding electron transfer steps are indicated by numbers. In the beginning, the PQ pool is almost completely reduced. This is observed as an elevated F_0 level which includes initial, natural F_0 and additional fluorescence from the high proportion of the closed PSII centers with Q_A^- present under these conditions (Fig. 11A). Immediately after the flash, the rest of the PSII centers (centers which were open before the flash) will also have Q_A reduced (Q_A^-) which is observed as F_m. Slow re-oxidation of Q_A^- is observed in those PSII centers immediately after the flash and represents a mixture of very slow forward electron transfer to Q_B which first have to bind to the Q_B site (phase I) and recombination to the donor side of PSII (phase IV). The slow decay phase I is observed as

a 'faux-plateau' and was described by us before (Volgusheva *et al.*, 2013, 2016).

Simultaneously, Cyt b_6/f is oxidizing the fraction of the PQ pool in the time range faster than 30 ms in the PSI-driven electron transfer, leading to the opening of the electron transfer from PSII. This opening is observed as a faster decay in the fluorescence kinetics and represents slow Q_A^- re-oxidation with a $t_{1/2}$ of 33 ms (phase II; Figs. 11A, B). This oxidation of the PQ pool is relatively efficient and results in drawdown of the fluorescence level below the initial (before flash) F_0 level, since there is an excess of active PSI centers over the decreased amount of PSII during the H_2-producing stage (Volgusheva *et al.*, 2013).

This partial oxidation of the PQ pool creates room for additional inflow of electrons from the reduced stromal components such as starch reserves or CEF, both mediated by NDA2. This electron inflow is observed as a fluorescence rise with a $t_{1/2}$ of 300 ms (phase III; Fig. 11A, B). It is observed as an increase in the variable fluorescence due to a shift in the redox equilibrium back to Q_A, again creating Q_A^- but this time in the dark [$Q_A^- \Leftarrow Q_B^- \Leftarrow$ PQ pool$^{(red)}$]. This increase in the fluorescence level overshoots above the initial (before flash) F_0 level, reaching the fluorescence level where the 'normal' Q_A^- re-oxidation under these conditions occurs (indicated by a dashed line; Fig. 11A). As a sum of these two reactions, slow Q_A^- re-oxidation (phases I and II; Fig. 11) and consequent Q_A reduction by NDA2 (III; Fig. 11), a transient dip in the fluorescence kinetics is observed at ~60 ms (Fig. 11A). After that a slow Q_A^- re-oxidation (phase II) is dominated by a recombination reaction within the PSII complex (phase IV; Fig. 11). Note that PTOXs active in chlororespiration are not functional due to the absence of O_2 as an electron acceptor under these conditions (Fig. 11B).

In the present study we show that the fluorescence wave phenomenon is a sensitive probe to the redox reactions during H_2 production in *C. reinhardtii*. For the first time, it provided information about the rates of electron transfer from the stromal components to the PQ pool during H_2 production. Potentially it can also serve as a measurement of the degree of the CEF and LEF in this process and to further characterize the NDA2-mediated electron transfer pathway in *C. reinhardtii*.

Acknowledgements

The authors would like to thank the Carl Tryggers Foundation for Scientific Research.

References

Alric J. 2014. Redox and ATP control of photosynthetic cyclic electron flow in *Chlamydomonas reinhardtii*: (II) involvement of the PGR5–PGRL1 pathway under anaerobic conditions. Biochimica et Biophysica Acta **1837**, 825–834.

Alric J. 2015. The plastoquinone pool, poised for cyclic electron flow? Frontiers in Plant Science **6**, 540.

Antal TK, Krendeleva TE, Laurinavichene TV, Makarova VV, Ghirardi ML, Rubin AB, Tsygankov AA, Seibert M. 2003. The dependence of algal H_2 production on Photosystem II and O_2 consumption activities in sulfur-deprived *Chlamydomonas reinhardtii* cells. Biochimica et Biophysica Acta **1607**, 153–160.

Antal TK, Krendeleva TE, Rubin AB. 2007. Study of photosystem 2 heterogeneity in the sulfur-deficient green alga *Chlamydomonas reinhardtii*. Photosynthesis Research **94**, 13–22.

Antal TK, Kukarskikh GP, Bulychev AA, Tyystjärvi E, Krendeleva T. 2013. Antimycin A effect on the electron transport in chloroplasts of two *Chlamydomonas reinhardtii* strains. Planta **237**, 1241–1250.

Antal T, Mattila H, Hakala-Yatkin M, Tyystjärvi T, Tyystjärvi E. 2010. Acclimation of photosynthesis to nitrogen deficiency in *Phaseolus vulgaris*. Planta **232**, 887–898.

Antal TK, Volgusheva AA, Kukarskih GP, Bulychev AA, Krendeleva TE, Rubin AB. 2006. Effects of sulfur limitation on photosystem II functioning in *Chlamydomonas reinhardtii* as probed by chlorophyll a fluorescence. Physiologia Plantarum **128**, 360–367.

Antal TK, Volgusheva AA, Kukarskih GP, Krendeleva TE, Rubin AB. 2009. Relationships between H_2 photoproduction and different electron transport pathways in sulfur-deprived *Chlamydomonas reinhardtii*. International Journal of Hydrogen Energy **34**, 9087–9094.

Arnon DI. 1949. Copper enzymes in isolated chloroplasts. Polyphenoloxidase in *Beta vulgaris*. Plant Physiology **24**, 1–15.

Baltz A, Dang KV, Beyly A, Auroy P, Richaud P, Cournac L, Peltier G. 2014. Plastidial expression of type II NAD(P)H dehydrogenase increases the reducing state of plastoquinones and hydrogen photoproduction rate by the indirect pathway in *Chlamydomonas reinhardtii*. Plant Physiology **165**, 1344–1352.

Batie CJ, Kamin H. 1984. Electron transfer by ferredoxin:NADP$^+$ reductase. Rapid-reaction evidence for participation of a ternary complex. Journal of Biological Chemistry **259**, 11976–11985.

Batyrova KA, Tsygankov AA, Kosourov SN. 2012. Sustained hydrogen photoproduction by phosphorus-deprived *Chlamydomonas reinhardtii* cultures. International Journal of Hydrogen Energy **37**, 8834–8839.

Bishop NI. 1958. The influence of the herbicide, DCMU, on the oxygen-evolving system of photosynthesis. Biochimica et Biophysica Acta **27**, 205–206.

Cleland RE, Bendall DS. 1992. Photosystem I cyclic electron transport: measurement of ferredoxin-plastoquinone reductase activity. Photosynthesis Research **34**, 409–418.

Crofts AR, Baroli I, Kramer D, Taoka S. 1993. Kinetics of electron-transfer between Q(a) and Q(B) in wild-type and herbicide-resistant mutants of *Chlamydomonas reinhardtii*. Zeitschrift für Naturforschung C **48**, 259–266.

Crofts AR, Wraight CA. 1983. The electrochemical domain of photosynthesis. Biochimica et Biophysica Acta **726**, 149–185.

Deák Z, Sass L, Kiss E, Vass I. 2014. Characterization of wave phenomena in the relaxation of flash-induced chlorophyll fluorescence yield in cyanobacteria. Biochimica et Biophysica Acta **1837**, 1522–1532.

Deris ZZ, Akter J, Sivanesan S, Roberts KD, Thompson PE, Nation RL, Li J, Velkov T. 2014. A secondary mode of action of polymyxins against Gram-negative bacteria involves the inhibition of NADH-quinone oxidoreductase activity. Journal of Antibiotics **67**, 147–151.

Desplats C, Mus F, Cuiné S, Billon E, Cournac L, Peltier G. 2009. Characterization of Nda2, a plastoquinone-reducing type II NAD(P)H dehydrogenase in Chlamydomonas chloroplasts. Journal of Biological Chemistry **284**, 4148–4157.

Draber W, Tietjen K, Kluth JF, Trebst A. 1991. Herbicides in photosynthesis research. Angewandte Chemie **30**, 1621–1633.

Esposti MD. 1998. Inhibitors of NADH-ubiquinone reductase: an overview. Biochimica et Biophysica Acta **1364**, 222–235.

Evans MC, Sihra CK, Cammack R. 1976. The properties of the primary electron acceptor in the Photosystem I reaction centre of spinach chloroplasts and its interaction with P700 and the bound ferredoxin in various oxidation–reduction states. The Biochemical Journal **158**, 71–77.

Faraloni C, Torzillo G. 2010. Phenotypic characterization and hydrogen production in *Chlamydomonas reinhardtii* Q(B)-binding D1-protein mutants under sulfur starvation: changes in chl fluorescence and pigment composition. Journal of Phycology **46**, 788–799.

Feng Y, Li W, Li J, *et al*. 2012. Structural insight into the type-II mitochondrial NADH dehydrogenases. Nature **491**, 478–482.

Fouchard S, Hemschemeier A, Caruana A, Pruvost J, Legrand J, Happe T, Peltier G, Cournac L. 2005. Autotrophic and mixotrophic hydrogen photoproduction in sulfur-deprived Chlamydomonas cells. Applied and Environmental Microbiology **71**, 6199–6205.

Gaffron H, Rubin J. 1942. Fermentative and photochemical production of hydrogen in algae. Journal of General Physiology **26**, 219–240.

Ghirardi ML. 2015. Implementation of photobiological H_2 production: the O_2 sensitivity of hydrogenases. Photosynthesis Research **125**, 383–393.

Ghirardi ML, Posewitz MC, Maness PC, Dubini A, Yu J, Seibert M. 2007. Hydrogenases and hydrogen photoproduction in oxygenic photosynthetic organisms. Annual Review of Plant Biology **58**, 71–91.

Godaux D, Emoncls-Alt B, Berne N, Ghysels B, Alric J, Remacle C, Cardol P. 2013. A novel screening method for hydrogenase-deficient mutants in *Chlamydomonas reinhardtii* based on in vivo chlorophyll fluorescence and photosystem II quantum yield. International Journal of Hydrogen Energy **38**, 1826–1836.

Gorman DS, Levine RP. 1965. Cytochrome f and plastocyanin—their sequence in photosynthetic electron transport chain of *Chlamydomonas reinhardi*. Proceedings of the National Academy of Sciences, USA **54**, 1665–1669.

Guedeney G, Corneille S, Cuiné S, Peltier G. 1996. Evidence for an association of ndh B, ndh J gene products and ferredoxin-NADP-reductase as components of a chloroplastic NAD(P)H dehydrogenase complex. FEBS Letters **378**, 277–280.

Hankamer B, Lehr F, Rupprecht J, Mussgnug JH, Posten C, Kruse O. 2007. Photosynthetic biomass and H_2 production by green algae: from bioengineering to bioreactor scale-up. Physiologia Plantarum **131**, 10–21.

Happe T, Hemschemeier A, Winkler M, Kaminski A. 2002. Hydrogenases in green algae: do they save the algae's life and solve our energy problems? Trends in Plant Science **7**, 246–250.

Harris EH. 2001. Chlamydomonas as a model organism. Annual Review of Plant Physiology and Plant Molecular Biology **52**, 363–406.

Harris EH. 2009. The Chlamydomonas sourcebook: introduction to Chlamydomonas and its laboratory use. Oxford: Academic Press.

Healey FP. 1970. Hydrogen evolution by several algae. Planta **91**, 220–226.

Hemschemeier A, Fouchard S, Cournac L, Peltier G, Happe T. 2008. Hydrogen production by *Chlamydomonas reinhardtii*: an elaborate interplay of electron sources and sinks. Planta **227**, 397–407.

Horner DS, Heil B, Happe T, Embley TM. 2002. Iron hydrogenases—ancient enzymes in modern eukaryotes. Trends in Biochemical Sciences **27**, 148–153.

Houille-Vernes L, Rappaport F, Wollman FA, Alric J, Johnson X. 2011. Plastid terminal oxidase 2 (PTOX2) is the major oxidase involved in chlororespiration in Chlamydomonas. Proceedings of the National Academy of Sciences, USA **108**, 20820–20825.

Ishikita H, Knapp EW. 2003. Redox potential of quinones in both electron transfer branches of photosystem I. Journal of Biological Chemistry **278**, 52002–52011.

Jans F, Mignolet E, Houyoux PA, *et al*. 2008. A type II NAD(P) H dehydrogenase mediates light-independent plastoquinone reduction in the chloroplast of Chlamydomonas. Proceedings of the National Academy of Sciences, USA **105**, 20546–20551.

Johnson X, Alric J. 2013. Central carbon metabolism and electron transport in *Chlamydomonas reinhardtii*: metabolic constraints for carbon partitioning between oil and starch. Eukaryotic Cell **12**, 776–793.

Kosourov S, Patrusheva E, Ghirardi ML, Seibert M, Tsygankov A. 2007. A comparison of hydrogen photoproduction by sulfur-deprived *Chlamydomonas reinhardtii* under different growth conditions. Journal of Biotechnology **128**, 776–787.

Kosourov S, Tsygankov A, Seibert M, Ghirardi ML. 2002. Sustained hydrogen photoproduction by *Chlamydomonas reinhardtii*: effects of culture parameters. Biotechnology and Bioengineering **78**, 731–740.

Krause GH, Weis E. 1991. Chlorophyll fluorescence and photosynthesis—the basics. Annual Review of Plant Physiology and Plant Molecular Biology **42**, 313–349.

Kruse O, Hankamer B. 2010. Microalgal hydrogen production. Current Opinion in Biotechnology **21**, 238–243.

Kurisu G, Zhang H, Smith JL, Cramer WA. 2003. Structure of the cytochrome b6f complex of oxygenic photosynthesis: tuning the cavity. Science **302**, 1009–1014.

Li X, Zhang R, Patena W, *et al*. 2016. An indexed, mapped mutant library enables reverse genetics studies of biological processes in *Chlamydomonas reinhardtii*. The Plant Cell **28**, 367–387.

Makarova VV, Kosourov S, Krendeleva TE, Semin BK, Kukarskikh GP, Rubin AB, Sayre RT, Ghirardi ML, Seibert M. 2007. Photoproduction of hydrogen by sulfur-deprived *C. reinhardtii* mutants with impaired photosystem II photochemical activity. Photosynthesis Research **94**, 79–89.

Mamedov F, Stefansson H, Albertsson PA, Styring S. 2000. Photosystem II in different parts of the thylakoid membrane: a functional comparison between different domains. Biochemistry **39**, 10478–10486.

Mathews J, Wang GY. 2009. Metabolic pathway engineering for enhanced biohydrogen production. International Journal of Hydrogen Energy **34**, 7404–7416.

Maxwell K, Johnson GN. 2000. Chlorophyll fluorescence—a practical guide. Journal of Experimental Botany **51**, 659–668.

Melis A. 2007. Photosynthetic H_2 metabolism in *Chlamydomonas reinhardtii* (unicellular green algae). Planta **226**, 1075–1086.

Melis A, Zhang L, Forestier M, Ghirardi ML, Seibert M. 2000. Sustained photobiological hydrogen gas production upon reversible inactivation of oxygen evolution in the green alga *Chlamydomonas reinhardtii*. Plant Physiology **122**, 127–136.

Mignolet E, Lecler R, Ghysels B, Remacle C, Franck F. 2012. Function of the chloroplastic NAD(P)H dehydrogenase Nda2 for H_2 photoproduction in sulphur-deprived *Chlamydomonas reinhardtii*. Journal of Biotechnology **162**, 81–88.

Mogi T, Murase Y, Mori M, Shiomi K, Omura S, Paranagama MP, Kita K. 2009. Polymyxin B identified as an inhibitor of alternative NADH dehydrogenase and malate:quinone oxidoreductase from the Gram-positive bacterium *Mycobacterium smegmatis*. Journal of Biochemistry **146**, 491–499.

Mus F, Cournac L, Cardettini V, Caruana A, Peltier G. 2005. Inhibitor studies on non-photochemical plastoquinone reduction and H_2 photoproduction in *Chlamydomonas reinhardtii*. Biochimica et Biophysica Acta **1708**, 322–332.

Mus F, Dubini A, Seibert M, Posewitz MC, Grossman AR. 2007. Anaerobic acclimation in *Chlamydomonas reinhardtii*: anoxic gene expression, hydrogenase induction, and metabolic pathways. Journal of Biological Chemistry **282**, 25475–25486.

Ohta S, Miyamoto K, Miura Y. 1987. Hydrogen evolution as a consumption mode of reducing equivalents in green algal fermentation. Plant Physiology **83**, 1022–1026.

Peltier G, Aro EM, Shikanai T. 2016. NDH-1 and NDH-2 plastoquinone reductases in oxygenic photosynthesis. Annual Review of Plant Biology **67**, 55–80.

Peltier G, Cournac L. 2002. Chlororespiration. Annual Review of Plant Biology **53**, 523–550.

Philipps G, Happe T, Hemschemeier A. 2012. Nitrogen deprivation results in photosynthetic hydrogen production in *Chlamydomonas reinhardtii*. Planta **235**, 729–745.

Redding K, Cournac L, Vassiliev IR, Golbeck JH, Peltier G, Rochaix JD. 1999. Photosystem I is indispensable for photoautotrophic growth, CO_2 fixation, and H_2 photoproduction in *Chlamydomonas reinhardtii*. Journal of Biological Chemistry **274**, 10466–10473.

Renger G, Eckert HJ, Bergmann A, Bernarding J, Liu B, Napiwotzki A, Reifarth F, Eichler HJ. 1995. Fluorescence and spectroscopic studies of exciton trapping and electron-transfer in photosystem-II of higher plants. Australian Journal of Plant Physiology **22**, 167–181.

Rich PR, Madgwick SA, Moss DA. 1991. The interactions of duroquinol, DBMIB and NQNO with the chloroplast cytochrome-bf complex. Biochimica et Biophysica Acta **1058**, 312–328.

Roose JL, Frankel LK, Bricker TM. 2010. Documentation of significant electron transport defects on the reducing side of photosystem II upon removal of the PsbP and PsbQ extrinsic proteins. Biochemistry **49**, 36–41.

Rottenberg H, Koeppe RE 2nd. 1989. Mechanism of uncoupling of oxidative phosphorylation by gramicidin. Biochemistry **28**, 4355–4360.

Stannard JN, Horecker BL. 1948. The in vitro inhibition of cytochrome oxidase by azide and cyanide. Journal of Biological Chemistry **172**, 599–608.

Tolleter D, Ghysels B, Alric J, *et al*. 2011. Control of hydrogen photoproduction by the proton gradient generated by cyclic electron flow in *Chlamydomonas reinhardtii*. The Plant Cell **23**, 2619–2630.

Vass I, Kirilovsky D, Etienne AL. 1999. UV-B radiation-induced donor- and acceptor-side modifications of photosystem II in the cyanobacterium *Synechocystis* sp. PCC 6803. Biochemistry **38**, 12786–12794.

Volgusheva A, Kruse O, Styring S, Mamedov F. 2016. Changes in the photosystem II complex associated with hydrogen formation in sulfur deprived *Chlamydomonas reinhardtii*. Algal Research **18**, 296–304.

Volgusheva A, Kukarskikh G, Krendeleva T, Rubin A, Mamedov F. 2015. Hydrogen photoproduction in green algae *Chlamydomonas reinhardtii* under magnesium deprivation. RSC Advances **5**, 5633–5637.

Volgusheva A, Styring S, Mamedov F. 2013. Increased photosystem II stability promotes H_2 production in sulfur-deprived *Chlamydomonas reinhardtii*. Proceedings of the National Academy of Sciences, USA **110**, 7223–7228.

Volgusheva AA, Zagidullin VE, Antal TK, Korvatovsky BN, Krendeleva TE, Paschenko VZ, Rubin AB. 2007. Examination of chlorophyll fluorescence decay kinetics in sulfur deprived algae *Chlamydomonas reinhardtii*. Biochimica et Biophysica Acta **1767**, 559–564.

Wykoff DD, Davies JP, Melis A, Grossman AR. 1998. The regulation of photosynthetic electron transport during nutrient deprivation in *Chlamydomonas reinhardtii*. Plant Physiology **117**, 129–139.

Zhang L, Happe T, Melis A. 2002. Biochemical and morphological characterization of sulfur-deprived and H_2-producing *Chlamydomonas reinhardtii* (green alga). Planta **214**, 552–561.